$MTi_{0.7}Mo_{0.3}Mo_5O_{10}$ (M = Sr, Eu), First Evidence of Mono- and Bicapped Bioctahedral Mo_{11} and Mo_{12} Clusters: Synthesis, Crystal Structures, and Physical Properties

J. Tortelier and P. Gougeon*

Laboratoire de Chimie du Solide et Inorganique Moléculaire, UMR 6511 CNRS-Université de Rennes 1, Institut de Chimie de Rennes, Avenue du Général Leclerc, 35042 Rennes Cedex, France

R. Gautier

Département de Physicochimie UPRES 1795, Ecole Nationale Supérieure de Chimie de Rennes, Institut de Chimie de Rennes, 35700 Rennes, France

R. Berjoan

I.M.P.-C.N.R.S. B.P. 5, 66125 ODEILLO, France

Received November 1, 2000

The novel quaternary reduced molybdenum oxides $MTi_{0.7}Mo_{0.3}Mo_5O_{10}$ (M = Sr, Eu) have been synthesized by solid-state reaction at 1400 °C for 48 h in sealed molybdenum crucibles. Their crystal structures were determined on single crystals by X-ray diffraction. Both compounds crystallize in the orthorhombic space group *Pbca* with 8 formula units per cell and the following lattice parameters: $a_{Sr} = 9.1085$ (7), $b_{Sr} = 11.418$ (1), and $c_{Sr} = 15.092$ (3) Å; $a_{Eu} = 9.1069$ (7), $b_{Eu} = 11.421$ (2), and $c_{Eu} = 15.075$ (1) Å. The Mo network is dominated by bioctahedral Mo_{10} clusters, which coexist randomly with Mo_{11} and Mo_{12} clusters (monocapped and bicapped Mo_{10} clusters). The Mo−Mo distances within the clusters range from 2.62 to 2.92 Å and the Mo−O distances from 1.99 to 2.17 Å as usually observed in the reduced molybdenum oxides. The Sr^{2+} and Eu^{2+} ions occupy large cavities, which result from the fusion of two cubooctahedra and thus are surrounded by 11 oxygen atoms. The M−O distances range from 2.50 to 3.23 Å for the Sr compound and from 2.49 to 3.24 Å for the Eu analogue. Single-crystal resistivity measurements indicate that both materials are poor metals with transitions to semiconducting states below 50 and 40 K and room temperature resistivity values of 9×10^{-3} and 5×10^{-3} Ω·cm for the Sr and Eu compounds, respectively. The magnetic susceptibility data indicate paramagnetic behavior due to the Eu^{2+} moment at high temperatures for the Eu compound and do not reveal the existence of localized moments on the Mo and Ti sublattice in the Sr compound. An XPS study clearly suggests that the isolated Ti ions are tetravalent. Theoretical considerations preclude the existence of heterometallic Mo−Ti clusters.

Introduction

A wide array of Mo−Mo bonded cluster types are found in the reduced oxides of molybdenum.[1] A common structural unit is the Mo_6 octahedron that occurs quasi-isolated in $Ca_{16.5}Mo_{13.5}O_{40}$[2] and $LaMo_2O_5$[3] or fused through edges to other such clusters to form larger entities of general formula Mo_{4n+2} in the series $M_{n-x}Mo_{4n+2}O_{6n+4}$ ($n = 2$,[4] 3,[5] 4,[6] and 5[7]). The range of clusters can also be extended by capping the faces of the Mo_6 octahedron to produce Mo_7 and Mo_8 clusters. The existence of the latter two clusters was first mentioned by Leligny et al. in the compound $LaMo_{7.7}O_{14}$[8] in which both clusters coexist randomly. Subsequently, both types of clusters were found in well-ordered structures. Thus, the monocapped octahedral Mo_7 has been observed up to now either forming infinite chains with bioctahedral Mo_{10} or quasi-isolated in the series of compounds $M_4M'_3Mo_{26}O_{48}$ (M = Sr, Eu, M′ = Al, Ga, Fe).[9] The bicapped octahedral Mo_8 cluster was encountered in the two isomeric

(1) Chippindale, A. M.; Cheetham, A. K. The Oxide Chemistry of Molybdenum. In *Studies in Organic Chemistry. Molybdenum: An Outline of its Chemistry and Uses*; Braitthwaite, E. R., Haber, T., Eds.; Elsevier: Amsterdam, The Netherlands, 1994.
(2) Lindblom, B.; Strandberg, R. *Acta Chem. Scand.* **1989**, *43*, 825.
(3) Hibble, S. J.; Cooper, S. P.; Hannon, A. C.; Patat, S.; McCarroll, W. H. *Acta Crystallogr.* **1997**, *B53*, 604.
(4) (a) Hibble, S. J.; Cheetham, A. K.; Bogle, A. R. L.; Wakerley, H. R.; Cox, D. E. *J. Am. Chem. Soc.* **1988**, *110*, 3295. (b) Dronskowski, R.; Simon, A. *Angew. Chem., Int. Ed. Engl.* **1989**, *28*, 758. (c) Gougeon, P.; Potel, M.; Sergent, M. *Acta Crystallogr.* **1990**, *C46*, 1188. (d) Gougeon, P.; Gall, P.; Sergent, M. *Acta Crystallogr.* **1991**, *C47*, 421. (e) Dronskowski, R.; Simon, A.; Mertin, W. *Z. Anorg. Allg. Chem.* **1991**, *602*, 49. (f) Gall, P.; Gougeon, P. *Acta Crystallogr.* **1994**, *C50*, 7. (g) Gall, P.; Gougeon, P. *Acta Crystallogr.* **1994**, *C50*, 1183.
(5) (a) Dronskowski, R.; Simon, A.; Mertin. W. *Z. Anorg. Allg. Chem.* **1991**, *602*, 49. (b) Dronskowski, R.; Simon, A. *Acta Chem. Scand.* **1991**, *45*, 850. (c) Schimek, G. L.; Chen, S. C.; McCarley, R. E. *Inorg. Chem.* **1995**, *34*, 6130.
(6) Schimek, G. L.; Nagaki, D. A.; McCarley, R. E. *Inorg. Chem.* **1994**, *33*, 1259.
(7) (a) Dronskowski, R.; Mattausch, H. J.; Simon, A. *Z. Anorg. Allg. Chem.* **1993**, *619*, 1397. (b) Schimek, G. L.; McCarley, R. E. *J. Solid State Chem.* **1994**, *113*, 345.
(8) Leligny, H.; Ledésert, M.; Labbé, Ph.; Raveau, B.; McCarroll, W. H. *J. Solid State Chem.* **1990**, *87*, 35−43.
(9) (a) Tortelier, J.; Gougeon, P. *Acta Crystallogr.* **1996**, *C52*, 1862. (b) Tortelier, J.; Gougeon, P.; Ramanujachary, K. V.; Greenblatt, M. *Mater. Res. Bull.* **1998**, *8*, 1151.

10.1021/ic001209g CCC: $20.00
Published on Web 04/12/2001

cis and trans forms in the series of polymorphic compounds RMo_8O_{14} (R = La, Ce, Pr, Nd, Sm)[10] compounds that were prepared by high-temperature solid-state reaction. Thus, in $NdMo_8O_{14}$[10a] and $SmMo_8O_{14}$,[10e] only cis-edge-sharing bi-face capped Mo_8 clusters are observed, while in $LaMo_8O_{14}$,[10d] $CeMo_8O_{14}$,[10b] and $PrMo_8O_{14}$[10c] well-ordered mixtures of cis-edge-sharing and trans bi-face capped octahedral Mo_8 clusters occur in equal proportion for the La and Ce compounds and in the ratio 2:1 for $PrMo_8O_{14}$. Another crystalline form of the stoichiometric $LaMo_8O_{14}$[11] compound was also synthesized by fused salt electrolysis. Its crystal structure is more complex due to a one-dimensional commensurate modulation and consists of cis-edge-sharing and trans bi-face capped Mo_8 clusters with an average probability distribution of approximately 65 and 35%, respectively. In addition to their fascinating structural aspects, the RMo_8O_{14} compounds present different magnetic behaviors resulting from the coexistence of two magnetic sublattices, one due to the rare-earth ions and the other one due to the clusters.[12]

In this work, we show how the face-capping principle can be extended to bioctahedral Mo_{10} units formed by fusing two Mo_6 clusters with the synthesis, crystal structures, and physical properties of the new compounds $MTi_{0.7}Mo_{0.3}Mo_5O_{10}$ (M = Sr and Eu) that contain the first examples of mono- and bicapped bioctahedral Mo_{11} and Mo_{12} clusters.

Experimental Section

Synthesis. The starting reagents were $SrMoO_4$ or Eu_2O_3 (Rhône-Poulenc, 99.999%), MoO_3 (Strem Chemicals, 99.9%), TiO_2 (Strem Chemicals, 99.99%), and Mo (Cime Bocuze, 99.99%), all in powder form. Before being used, the Mo powder was heated under a hydrogen flow at 1000 °C for 6 h and the rare-earth oxide was prefired at 1000 °C overnight and left at 600 °C before weighing it. Strontium molybdate was prepared by heating a stoichiometric mixture of strontium carbonate (Prolabo, 99%) and molybdenum trioxide in an open porcelain crucible at 800 °C overnight. All reactions were carried out in molybdenum crucibles which were previously cleaned by heating at about 1500 °C for 15 min under a dynamic vacuum of about 10^{-5} Torr. Single crystals of $EuTi_{0.7}Mo_{0.3}Mo_5O_{10}$ were first obtained in an attempt to prepare $Eu_4Ti_3Mo_{26}O_{48}$ which would lead to a compound isostructural with $Eu_4Ga_3Mo_{26}O_{48}$.[9] The exact composition was first determined by single-crystal X-ray structure investigations. Subsequently, X-ray pure powders of $EuTi_{0.7}Mo_{0.3}Mo_5O_{10}$ and $SrTi_{0.7}Mo_{0.3}Mo_5O_{10}$ could be obtained. For all syntheses, the mixtures of the starting materials were pressed into pellets and loaded into molybdenum crucibles which were sealed under a low argon pressure using an arc welding system. The crucibles were heated at 1500 °C for 48 h and then cooled at 100 °C/h down to 1100 °C, the temperature at which the furnace was shut off. Reactions carried out with different ratios Mo/Ti were also tested and did not lead to single-phase products. By substituting Ca for Sr and Eu, an isotructural compound could be observed. However single-phase preparation of this latter compound has not been achieved and only twinned single crystals of $CaTi_{0.7}Mo_{0.3}Mo_5O_{10}$ were obtained. On the other hand, attempts to synthesize isotructural compounds by substituting Ba, Sn, Pb, La, or Yb for Sr or Eu as well as Sc, V, Cr, Fe, Co, Ge, Zr, Al, and Si for Ti were not successful over a range of temperatures and times, 1400−1600 °C and 24−48 h, respectively.

The purity of the Sr and Eu compounds was checked on the basis of their X-ray powder diffraction patterns carried out on an Inel position sensitive detector with a 0 to 120° 2θ aperture and Cu Kα_1 radiation.

Table 1. X-ray Crystallographic and Experimental Data for $M(Ti_{0.7}Mo_{0.3})Mo_5O_{10}$ (M = Sr, Eu)

formula	$EuTi_{0.698(3)}Mo_{0.302(3)}Mo_5O_{10}$	$SrTi_{0.701(4)}Mo_{0.299(4)}O_{10}$
fw, g mol^{-1}	853.97	789.63
space group	*Pbca* (No. 61)	
a, Å	9.1069 (7)	9.1085 (7)
b, Å	11.421 (2)	11.418 (1)
c, Å	15.075 (1)	15.092 (3)
V, Å^3	1567.9 (3)	1569.6 (4)
Z	8	
ρ_{calcd}, g cm^{-3}	7.235	6.683
T, °C	20	
λ, Å	0.71073 (Mo Kα)	
μ, cm^{-1}	16.800	15.661
R_1[a] ($I > 2\sigma(I)$)	0.0347	0.0357
wR_2[b] (on all data)	0.0868	0.0771

[a] $R_1 = \Sigma||F_o| - |F_c||/\Sigma|F_o|$. [b] $wR_2 = \{\Sigma[w(F_o^2 - F_c^2)^2]/\Sigma[w(F_o^2)^2]\}^{1/2}$, $w = 1/[\sigma^2(F_o^2) + (aP)^2 + bP]$ where $P = [\max(F_o^2,0) + 2F_c^2]/3$ and $a =$ 0.0163 and 0.0297, and $b =$ 43.4046 and 0.0 for the Eu and Sr compounds, respectively.

We have summarized in Table 1 the lattice parameters of the $MTi_{0.7}Mo_{0.3}Mo_5O_{10}$ compounds. The latter were determined by least squares refinement of the setting angles of 25 reflections in the 2θ range 10−34° that had been automatically centered on a Nonius CAD4 diffractometer. Both compounds crystallize in the orthorhombic space group *Pbca* with 8 formulae per unit cell.

Single-Crystal Structure Determinations. The crystal structure was first established from intensity data collected on a single crystal of $EuTi_{0.7}Mo_{0.3}Mo_5O_{10}$. A black single crystal of approximate dimensions $0.2 \times 0.16 \times 0.14$ mm^3 with irregular shape was selected for data collection. Intensity data were recorded up to $\theta = 45°$ with the $\omega-2\theta$ scan method on a CAD4 Nonius diffractometer using graphite-monochromatized MoKα radiation ($\lambda = 0.71073$ Å) at room temperature. The intensities of three standard reflections showed no significant variations over the data collection. The data set was corrected for Lorentz and polarization effects and for absorption by employing the Ψ scan method[13] on six reflections. Analysis of the data revealed that the systematic absences (0*kl*) $k = 2n + 1$, (*h*0*l*) $l = 2n + 1$, and (*hk*0) $h = 2n + 1$ were consistent with the orthorhombic space group *Pbca*. The initial positions for all the molybdenum and some of the oxygen atoms as well as for the europium atom were determined with the direct methods program SHELXS[14] in the *Pbca* space group. A subsequent difference Fourier synthesis revealed the remaining oxygen atoms and two peaks M1 and M2 at 0.36 Å from each other, which we assigned to titanium atoms. Refinement of this model including the isotropic displacement parameters and the site occupancy factors for the titanium atoms showed that the latter ones were greater than unity. In the following step of the refinement, the occupation of the M1 and M2 sites by titanium and molybdenum atoms was taken into account. These refinements revealed that the M1 site [$x = 0.3618$, $y = 0.1810$, $z = 0.7036$] was only partially occupied by the titanium and the M2 site [$x = 0.3844$, $y = 0.2949$, $z = 0.1960$] by the molybdenum. A calculation of the two Mo6 and Ti probability density functions shows that they do not overlap and that for both atoms the position of the density maximum coincides with the refined position. The final full-matrix least squares refinement on F^2 which was based on a model including the positional and anisotropic displacement parameters for all atoms and site occupancy factors for Ti and Mo6 led to the values of $R = 0.0347$ and $wR = 0.0843$ for 5286 reflections with $I > 2\sigma(I)$ and to the stoichiometry $EuTi_{0.698(3)}Mo_{0.302(3)}Mo_5O_{10}$. As some atoms (Mo2 and Mo3) showed relatively high maximum and minimum main axis atomic displacement parameter (ADP) ratios of about 4, attempts were made to split the positions of the Mo2 and Mo3 atoms. Refinements of the latter model did not improve the results and led to a higher ratio for the Mo2 atoms. On the other hand, refinements in the four possible

(10) (a) Gougeon, P.; McCarley, R. E. *Acta Crystallogr.* **1991**, *C47*, 241. (b) Kerihuel, G.; Gougeon, P. *Acta Crystallogr.* **1995**, *C51*, 787. (c) Kerihuel, G.; Gougeon, P. *Acta Crystallogr.* **1995**, *C51*, 1475. (d) Kerihuel, G.; Tortelier, J.; Gougeon, P. *Acta Crystallogr.* **1996**, *C52*, 2389. (e) Tortelier, J.; Gougeon, P. *Acta Crystallogr.* **1997**, *C53*, 668.
(11) Leligny, H.; Labbé, Ph.; Ledesert, M.; Hervieu, M.; Raveau, B; McCarroll, W. H. *Acta Crystallogr.* **1993**, *B49*, 444.
(12) Gautier, R.; Andersen, O. K.; Gougeon, P.; Halet, J.-F.; Canadell, E. Unpublished results.
(13) North, A. C. T.; Phillips, D. C.; Mathews, F. S. *Acta Crystallogr.* **1968**, *A24*, 351.
(14) Sheldrick, G. M. *Acta Crystallogr.* **1990**, *A46*, 467.

Table 2. Positional Parameters and Equivalent Isotropic Displacement Parameters (Å^2) for $M(Ti_{0.7}Mo_{0.3})Mo_5O_{10}$ (M = Sr, Eu)

atom	*x*	*y*	*z*	U_{eq}	τ
			M = Sr		
Sr	0.49231(4)	0.58819(4)	0.10031(3)	0.00903(7)	1
Mo1	0.62235(3)	0.17780(3)	0.13465(2)	0.00531(5)	1
Mo2	0.38613(3)	0.05384(3)	0.18738(2)	0.00559(5)	1
Mo3	0.37347(3)	0.17186(3)	0.02651(2)	0.00393(5)	1
Mo4	0.63259(3)	0.93730(3)	0.12598(2)	0.00398(5)	1
Mo5	0.12555(3)	0.43492(3)	0.02739(2)	0.00340(5)	1
Mo6	0.3844(2)	0.29487(18)	0.19601(15)	0.0040(3)	0.299(4)
Ti	0.3618(2)	0.18101(17)	0.70365(13)	0.0043(2)	0.701(4)
O1	0.2633(3)	0.4394(2)	0.81056(18)	0.0053(4)	1
O2	0.9907(3)	0.1945(3)	0.9122(2)	0.0095(5)	1
O3	0.2560(3)	0.3089(2)	0.96976(19)	0.0065(4)	1
O4	0.0026(4)	0.3193(2)	0.7539(2)	0.0132(6)	1
O5	0.2543(3)	0.1934(2)	0.80667(18)	0.0059(4)	1
O6	0.9880(3)	0.0671(2)	0.7456(2)	0.0059(5)	1
O7	0.2537(3)	0.1829(2)	0.14161(19)	0.0069(5)	1
O8	0.2570(3)	0.4357(2)	0.14006(19)	0.0064(5)	1
O9	0.5031(3)	0.1938(2)	0.91801(18)	0.0048(4)	1
O10	0.2190(3)	0.0519(3)	0.97933(18)	0.0052(4)	1
			M = Eu		
Eu	0.49232(2)	0.58821(2)	0.099944(16)	0.00675(4)	1
Mo1	0.62262(4)	0.17763(3)	0.13469(2)	0.00276(5)	1
Mo2	0.38616(4)	0.05371(3)	0.18744(2)	0.00309(5)	1
Mo3	0.37373(4)	0.17202(3)	0.02656(2)	0.00143(5)	1
Mo4	0.63238(4)	0.93722(3)	0.12606(2)	0.00150(5)	1
Mo5	0.12546(4)	0.43497(3)	0.02737(2)	0.00096(5)	1
Mo6	0.3843(2)	0.29522(18)	0.19614(9)	0.00200(12)	0.302(3)
Ti	0.36167(17)	0.18079(16)	0.70342(8)	0.00200(12)	0.698(3)
O1	0.2630(4)	0.4398(3)	0.8100(2)	0.0038(4)	1
O2	0.9909(4)	0.1947(3)	0.9124(2)	0.0070(5)	1
O3	0.2561(3)	0.3094(3)	0.9697(2)	0.0030(4)	1
O4	0.0022(4)	0.3187(3)	0.7544(3)	0.0097(6)	1
O5	0.2547(4)	0.1933(3)	0.8067(2)	0.0039(4)	1
O6	0.9879(3)	0.0663(3)	0.7455(2)	0.0032(4)	1
O7	0.2536(4)	0.1829(3)	0.1416(2)	0.0044(4)	1
O8	0.2569(4)	0.4350(3)	0.1399(2)	0.0042(4)	1
O9	0.5038(3)	0.1943(3)	0.91776(19)	0.0025(4)	1
O10	0.2205(3)	0.0521(3)	0.9790(2)	0.0033(4)	1

orthorhombic subgroups $Pbc2_1$, $Pb2_1a$, and $P2_1ca$, and $P2_12_12_1$ were also unsuccessful. These slightly high values of the maximum and minimum main axis ADP ratios probably result from the disorder on the capping site Mo6. Refinements of the occupancy factors for the Eu cationic site yielded a value of 0.99 (2) and showed that it is fully occupied. Fractional coordinates of the Eu compound were used as starting values for the refinement of the Sr analogue. The final refinement ($R = 0.0357$ and $wR = 0.0682$ for 3493 reflections with $I > 2\sigma(I)$) led to the chemical formula $SrTi_{0.701(4)}Mo_{0.299(4)}Mo_5O_{10}$. For the Sr compound, the stoichiometry found from the refinement was consistent with that obtained by chemical analysis using a Bair Atomic inductively coupled plasma emission spectrometer (ICP) on a batch of 20 mg of crystals that yielded $Sr_{0.98(1)}Ti_{0.72(4)}Mo_{5.28(4)}O_{10}$. Because of the disordering of the Mo6 and Ti atoms and the absence of a solid solution Mo/Ti, we made long-exposure rotation photographs along the three crystallographic axes on a single crystal of $EuTi_{0.7}Mo_{0.3}Mo_5O_{10}$. The latter did not reveal any superlattice reflection. Calculations were performed on a Pentium II 450 for SHELXS and SHELXL-93[15] and on a Digital microVAX 3100 for the MolEN[16] programs (data reduction and absorption corrections). The crystallographic and experimental data are summarized in Table 1. The final atomic coordinates and temperature factors are reported in Table 2 and selected interatomic distances in Table 3.

Electrical Resistivity Measurements. The ac resistivity measurement was carried out on a single crystal using a standard four-probe technique between 290 and 4.2 K with a current amplitude of 1 mA and a frequency of 80 Hz. Ohmic contacts were made by attaching molten indium ultrasonically. The voltage drops across the sample were recorded as a function of temperature. The temperature readings were provided by platinum resistance thermometers.

Table 3. Selected Mo−Mo, Mo−O, Ti−O, and M−O (Å) for $M(Ti_{0.7}Mo_{0.3})Mo_5O_{10}$ (M = Sr, Eu)

	Eu	Sr		Eu	Sr
Mo1−Mo2	2.6967(5)	2.6956(5)	Mo1−O3	1.994(3)	1.997(3)
Mo1−Mo6	2.715(2)	2.710(2)	Mo1−O4	2.000(4)	2.005(3)
Mo1−Mo4	2.7502(7)	2.7507(5)	Mo1−O2	2.017(4)	2.016(3)
Mo1−Mo5	2.7611(5)	2.7636(6)	Mo1−O1	2.032(3)	2.030(3)
Mo1−Mo3	2.7926(5)	2.7941(5)	Mo1−O5	2.098(3)	2.095(3)
Mo1−Ti	3.055(2)	3.052(2)			
			Mo2−O6	1.990(3)	1.998(3)
Mo2−Mo6	2.761(2)	2.755(2)	Mo2−O4	2.002(4)	2.002(3)
Mo2−Mo4	2.7666(5)	2.7692(5)	Mo2−O8	2.012(3)	2.008(3)
Mo2−Mo5	2.7700(5)	2.7722(6)	Mo2−O7	2.028(3)	2.026(3)
Mo2−Mo3	2.7786(5)	2.7792(6)	Mo2−O1	2.162(3)	2.171(3)
Mo2−Ti	3.050(2)	3.046(2)			
			Mo3−O9	2.039(3)	2.034(3)
Mo3−Mo4	2.6178(5)	2.6178(6)	Mo3−O7	2.054(3)	2.055(3)
Mo3−Mo5	2.7073(7)	2.7054(5)	Mo3−O2	2.074(3)	2.079(3)
Mo3−Mo5	2.7220(5)	2.7240(4)	Mo3−O10	2.083(3)	2.089(3)
Mo3−Mo6	2.920(2)	2.920(2)	Mo3−O3	2.084(3)	2.080(3)
Mo3−Ti	3.154(2)	3.159(2)	Mo4−O9	2.057(3)	2.052(3)
			Mo4−O9	2.057(3)	2.052(3)
Mo4−Mo3	2.6178(5)	2.6178(6)	Mo4−O5	2.076(3)	2.079(3)
Mo4−Mo5	2.7358(5)	2.7368(6)	Mo4−O10	2.078(3)	2.090(3)
Mo4−Mo1	2.7502(7)	2.7507(5)	Mo4−O1	2.078(3)	2.077(3)
Mo4−Mo2	2.7666(5)	2.7692(5)	Mo4−O6	2.108(3)	2.114(3)
Mo4−Mo5	2.7799(5)	2.7827(5)			
Mo4−Ti	2.903(2)	2.905(2)	Mo5−O9	2.023(3)	2.021(3)
Mo4−Mo6	3.136(2)	3.144(2)	Mo5−O3	2.056(3)	2.059(3)
			Mo5−O10	2.071(3)	2.077(3)
Mo5−Mo3	2.7073(6)	2.7054(5)	Mo5−O8	2.077(3)	2.080(3)
Mo5−Mo3	2.7220(5)	2.7240(4)			
Mo5−Mo4	2.7358(5)	2.7368(6)	Mo6−O4	1.844(5)	1.852(4)
Mo5−Mo1	2.7611(5)	2.7636(6)	Mo6−O2	1.906(4)	1.903(4)
Mo5−Mo2	2.7700(5)	2.7722(6)	Mo6−O7	1.934(4)	1.930(3)
Mo5−Mo4	2.7799(5)	2.7827(5)	Mo6−O6	2.041(3)	2.038(3)
Mo5−Mo5	2.8475(7)	2.8501(6)	Mo6−O5	2.046(4)	2.052(3)
			Mo6−O8	2.148(4)	2.155(3)
Mo6−Ti	0.360(2)	0.363(2)			
Mo6−Mo1	2.715(2)	2.710(2)	Ti−O5	1.842(3)	1.843(3)
Mo6−Mo2	2.761(2)	2.755(2)	Ti−O8	1.891(3)	1.899(3)
Mo6−Mo3	2.920(2)	2.920(2)	Ti−O6	1.903(3)	1.898(3)
Mo6−Mo4	3.136(2)	3.144(2)	Ti−O7	2.064(4)	2.064(3)
			Ti−O2	2.111(4)	2.112(4)
Ti−Mo6	0.360(2)	0.363(2)	Ti−O4	2.126(5)	2.133(4)
Ti−Mo4	2.903(2)	2.905(2)			
Ti−Mo2	3.050(2)	3.046(2)	M−O9	2.498(3)	2.504(3)
Ti−Mo1	3.055(2)	3.052(2)	M−O4	2.561(4)	2.548(4)
Ti−Mo3	3.154(2)	3.159(2)	M−O7	2.565(3)	2.565(3)
			M−O1	2.629(3)	2.620(3)
			M−O10	2.693(3)	2.685(3)
			M−O3	2.778(3)	2.784(3)
			M−O8	2.832(3)	2.826(3)
			M−O10	2.881(3)	2.875(3)
			M−O6	2.923(3)	2.925(3)
			M−O2	3.082(4)	3.091(3)
			M−O2	3.241(3)	3.233(3)

Magnetic Susceptibility Measurements. Magnetic susceptibility data were collected on a SHE-906 SQUID magnetosusceptometer in the temperature range 5−300 K under a magnetic field of 4 kGauss. The measurements were carried out on cold pressed powder samples (ca. 150 mg). Data were corrected from the diamagnetism of the sample holder prior to analysis.

XPS Study. The oxide samples were analyzed by XPS experiments which were done in a CAMECA RIBER model SIA 200 electron spectrometer for multitechnique surface analysis. This system was equipped with a MAC 2 CAMECA RIBER double stage cylindrical mirror electron energy analyzer. The photon source was a CAMECA

(15) Sheldrick, G. M. SHELXL93, *Program for theRefinement of Crystal Structures*, University of Göttingen, Germany, 1993.
(16) Fair, C. K. MolEN, *An Interactive Intelligent System for Crystal Structure Analysis*; Enraf-Nonius, Delft Instruments X-ray Diffraction BV, Rontgenweg 1, 2624 BD Delft, The Netherlands, 1990.

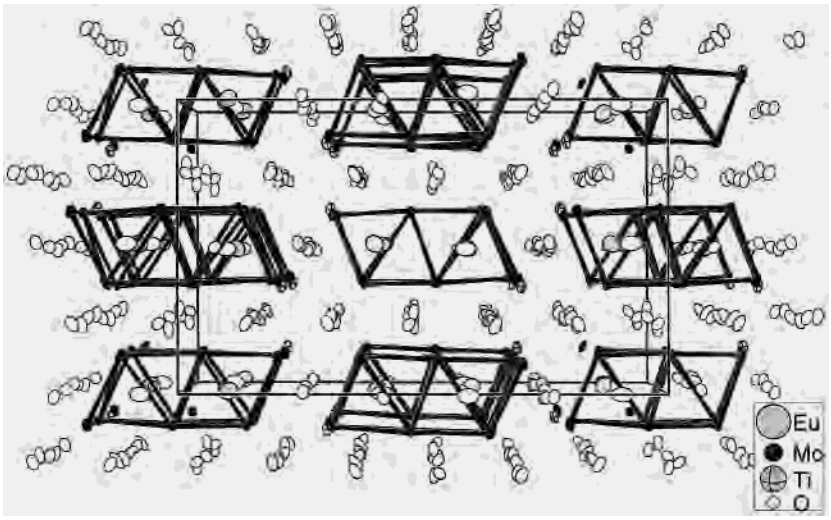

Figure 1. Perspective view of the crystal structure of $MTi_{0.7}Mo_{0.3}Mo_5O_{10}$ (M = Sr, Eu) along the *b* axis.

SCX 700 dual anode X-ray source. A nonmonochromatized Al Kα X-ray source ($h\nu = 1486.6$ eV) was used as the excitation source in all cases. Spectrometer energy calibration was carried out by use of the Au $4f_{7/2}$ and the Cu $2p_{3/2}$ photoelectron lines. The oxide samples were analyzed either without ion sputtering or after ion sputtering with 0.6 keV Ar^+ ions for 10 min. The oxidation state for titanium was examined from the Ti 2p core level binding energy chemical shift observed before and after ion sputtering.

Extended Hückel Calculations. Calculations have been carried out within the extended Hückel formalism[17] using the weighted H_{ij} formula[18] with the program CACAO.[19] The exponents (ξ) and the valence shell ionization potentials (H_{ii} in eV) were (respectively) as follows: 2.275, −32.3 for O 2s; 2.275, −14.8 for O 2p; 1.075, −8.97 for Ti 4s; 0.675, −5.44 for Ti 4p; 1.956, −8.34 for Mo 5s; 1.921, −5.24 for Mo 5p. H_{ii} values for Ti 3d and Mo 4d were set equal to −10.81 and −10.50, respectively. A linear combination of two Slater-type orbitals of exponents $\zeta_1 = 4.550$ and $\zeta_2 = 1.400$ with the weighting coefficients $c_1 = 0.4206$ and $c_2 = 0.7839$, and $\zeta_1 = 4.542$ and $\zeta_2 = 1.901$ with equal weighting coefficients, was used to represent the Ti 3d and Mo 4d atomic orbitals, respectively.

Results and Discussion

A perspective view of the crystal structure of $MTi_{0.7}Mo_{0.3}Mo_5O_{10}$ along the *b* axis is shown in Figure 1. The oxygen framework derives from a stacking along the *a* direction of close-packed layers with the sequence ...ABAC.... While the B ($y \approx 0.25$) and C ($y \approx 0.75$) layers are entirely occupied by oxygen atoms and have the composition [O_{24}], in the A layers ($y \approx 0.0$ and 0.5) one-third of the oxygen atoms are missing or substituted by the Sr or Eu ions in an ordered way. The latter layers can be thus formulated [O16 M4□4] where M stands for Eu or Sr and □ for the oxygen vacancies. Within the O network, half of the octahedral interstices are occupied by the Mo1, Mo2, Mo3, Mo4, and Mo5 atoms which form bioctahedral Mo_{10} clusters and one-tenth statistically by the Mo6 and Ti atoms. The bioctahedral Mo_{10} clusters occurring in these new mixed titanium molybdates result from the metal-edge condensation of two octahedral Mo_6-type clusters and are similar to those previously observed in the series of compounds MMo_5O_8 (M = Ca, Sr, La to Gd, Sn, and Pb)[4] where they form infinite chains and in the $R_{16}Mo_{21}O_{56}$ (R = La, Ce, Pr, and Nd)[20] compounds where they coexist with single MoO_6 octahedra. It is also

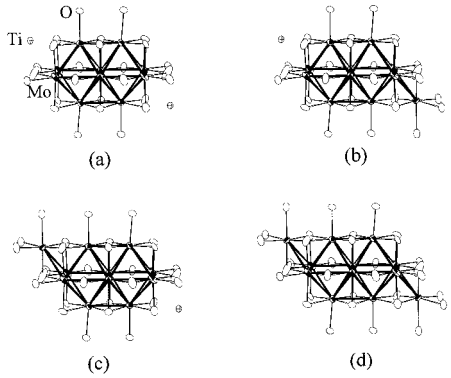

Figure 2. Four possible configurations for the Mo and Ti arrangement: (a) $Mo_{10}O_{18}$ unit, (b) and (c) $Mo_{11}O_{18}$ unit, and (d) $Mo_{12}O_{18}$ unit.

interesting to note that the vacancies in the A layers correspond to the center of the octahedra forming the Mo_{10} clusters. Obviously, because the Mo6 and Ti sites cannot be occupied simultaneously since they are separated only by 0.36 Å, only four different configurations which are described in Figure 2 are plausible. An examination of the distances between the Mo atoms forming the Mo_{10} clusters and the Mo6 atoms revealed that they agree well with the existence of metallic bonds: 2.71 Å for Mo6−Mo1, 2.76 Å for Mo6−Mo2, and 2.92 Å for Mo6−Mo3 (see Figure 4). The latter long Mo−Mo distance corresponds to a weak bond and is explained by the alternating short and long distances that are always observed between the apical Mo atoms in the polyoctahedral Mo_{4n+2} clusters.[21] This leads to the formation of monocapped and bicapped bioctahedral Mo_{11} and Mo_{12} clusters (Figures 2b−d). Both clusters which are new to solid-state chemistry coexist randomly with the Mo_{10} clusters in the $MTi_{0.7}Mo_{0.3}Mo_5O_{10}$ compounds. Moreover, the distances between the Mo_{10} clusters and the Ti atoms, which are greater than 2.9 Å, preclude the presence of heteronuclear clusters such as $Mo_{10}Ti$ or $Mo_{10}Ti_2$. Recent theoretical calculations performed on the bioctahedral Mo_{10} cluster occurring in the $La_{16}Mo_{21}O_{56}$[20c] and MMo_5O_8[22] compounds have shown that the maximum of electrons that the Mo_{10} cluster can accommodate is 30 and that higher electron counts per Mo_{10} cluster lead to the formation of short intercluster Mo−Mo bonds of

(17) Hoffmann, R. *J. Chem. Phys.* **1963**, *39*, 1397.
(18) Ammeter, J. H.; Bürgi, H.-B.; Thibeault, J. C.; Hoffmann, R. *J. Am. Chem. Soc.* **1978**, *100*, 3686.
(19) Mealli, C.; Proserpio, D. *J. Chem. Educ.* **1990**, *67*, 399.
(20) (a) Gall, P.; Gougeon, P. *Acta Crystallogr.* **1993**, *C49*, 659. (b) Gall, P.; Gougeon, P. *Z. Kristallogr.* **1998**, *213*, 1. (c) Gall, P.; Gautier, R.; Halet, J.-F.; Gougeon; P. *Inorg. Chem.* **1999**, *38*, 4455.
(21) Wheeler, R. A.; Hoffmann, R. *J. Am. Chem. Soc.* **1988**, *110*, 7315.

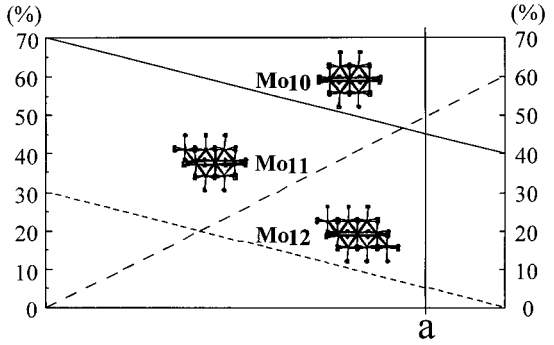

Figure 3. Different possible distributions of the Mo_{10}, Mo_{11}, and Mo_{12} clusters in the $M(Ti_{0.7}Mo_{0.3})Mo_5O_{10}$ (M = Eu. Sr) compounds. The percentage of each cluster type is given by the intersection of the corresponding curve with a given line parallel to the *y* axis. For example, we have 45, 50, and 5% of Mo_{10}, Mo_{11}, and Mo_{12} clusters, respectively, for the line a.

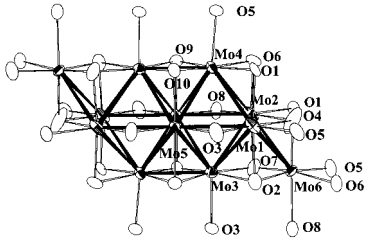

Figure 4. Numbering scheme used for the Mo−O clusters.

about 2.7 Å as observed in the series MMo_5O_8 (32 e^- per Mo_{10} cluster) and RMo_5O_8 (34 e^- per Mo_{10} cluster) (M = divalent metal and R = trivalent metal). In the $MTi_{0.7}Mo_{0.3}Mo_5O_{10}$ compounds, if we assume that the Mo6 and Ti are tetravalent (vide infra), we would have 32 e^- per Mo_{10} cluster. As we do not observe short Mo−Mo bonds between the Mo_{10} clusters, this implies the existence of some Mo−Mo bonds between the Mo_{10} clusters and the Mo6 atoms. A study of the capping effect of the Mo_{10} cluster by Mo or Ti atoms using extended Hückel calculations reveals that frontier orbitals of the capping MeO_3 group (Me = Mo, Ti) interact with antibonding vacant molecular orbitals (MO) of the Mo_{10} cluster. This is in contradiction with the capping principle established by Mingos which has been successful in rationalizing the bonding mode in capped late-transition metal organometallic clusters.[23] The resulting in-phase MO lie above the 15 bonding levels of the Mo_{10} unit. The absence of significant HOMO/LUMO gaps in the MO diagram of $MeMo_{10}$ and Me_2Mo_{10} clusters (Me = Ti, Mo) makes it difficult to establish favored electron counts for these units. Anyway, bonding between metallic atoms of the Mo_{10} cluster and the capping group occurs if these Me−Mo_{10} bonding levels are occupied. Considering the +4 oxidation state of the capping metal, the Ti atom has no more electrons whereas the Mo atom has 2 electrons left for the bonding with the Mo_{10} units. This is consistent with the crystallographic metal−metal distances between the capping metal and the metal atoms of the Mo_{10} units. Consequently, the existence of new Mo_{11} and Mo_{12} clusters must be envisioned and the presence of heteronuclear clusters such as $Mo_{10}Ti$ or $Mo_{10}Ti_2$ must be excluded.

In Figure 3, we show the possible distributions of the three different clusters, which vary between 40% of Mo_{10} and 60% of Mo_{11} and 70% of Mo_{10} and 30% of Mo_{12}. It is also interesting to mention that the random combination of Mo clusters of different sizes has already been observed for $LaMo_{7.7}O_{14}$[8] in which monocapped Mo_7 and bicapped Mo_8 octahedral clusters coexist. Figure 4 shows the numbering scheme used for the molybdenum oxide clusters. The Mo−Mo distances within the Mo_{10} clusters range from 2.62 to 2.85 Å with a mean value of 2.74 Å for the two isostructural Sr and Eu compounds. The smaller distance occurs between the apical Mo3 and Mo4 atoms and the larger one between the Mo5 atoms of the shared edge. If we except the capping Mo6 atoms of the Mo_{11} and Mo_{12} clusters that are coordinated octahedrally by oxygen atoms and the Mo5 atoms of the shared edge that are surrounded by four oxygen atoms, the other Mo atoms are in a square pyramidal environment of oxygen atoms. The Mo−O bond distances are in the range 1.85−2.17 Å as usually observed in reduced molybdenum oxides.

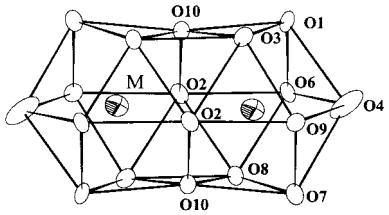

M = Sr, Eu

Figure 5. Environments of the cation M in the $M(Ti_{0.7}Mo_{0.3})Mo_5O_{10}$ (M = Eu, Sr) compounds.

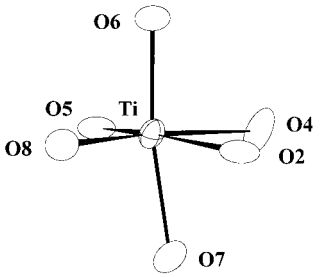

Figure 6. Environment of the titanium in the $M(Ti_{0.7}Mo_{0.3})Mo_5O_{10}$ (M = Eu, Sr) compounds.

The Sr^{2+} and Eu^{2+} ions occupy large cavities, which result from the fusion of two cubooctahedra and thus are surrounded by 11 oxygen atoms (Figure 5). The M^{2+}−O distances range from 2.504 (3) to 3.233 (3) Å (mean value 2.787 Å) and from 2.498 (3) to 3.241 (3) Å (mean value 2.789 Å) for the Sr and Eu compounds, respectively. The Ti atoms are surrounded by six oxygen atoms forming a highly distorted octahedron (Figure 6). The Ti−O distances range between 1.9 and 2.06 Å with a mean value of 1.98 Å. From the Ti−O bond lengths, the valence of the Ti atoms calculated by using the relationship of Brown and Wu [$(s = (d_{Ti-O}/1.806)^{-5.2})$][24] is +3.8, suggesting a number of oxidation of +4. The tetravalence of the titanium was confirmed by XPS measurements, which show two peaks at 459 and 465 eV for the Ti $2p_{3/2}$ and Ti $2p_{1/2}$ binding energies, respectively (Figure 7). For Ti^{3+}, the observed Ti $2p_{3/2}$ binding energy lies generally in the range 455.2 to 458 eV and the Ti $2p_{1/2}$ one between 463 and 463.5 eV, while for Ti^{4+} the Ti $2p_{3/2}$ binding energy varies between 458.5 and 459 eV and the Ti $2p_{1/2}$ one between 464.5 and 465 eV.

The temperature dependencies of the molar magnetic susceptibility of $SrTi_{0.7}Mo_{0.3}Mo_5O_{10}$ and of the inverse of the molar

(22) Koo, H.-J.; Whangbo, M.-H.; McCarroll, W. H.; Greenblatt, M.; Gautier, R.; Halet, J.-F.; Gougeon, P. *Solid State Commun.* **1998**, *8*, 539.

(23) Mingos, D. M. P.; Wales, D. J. *Introduction to Cluster Chemistry*; Prentice-Hall: New Jersey, 1990.

(24) Brown, I. D.; Wu, K. K. *Acta Crystallogr*. **1976**, *B32*, 1957.

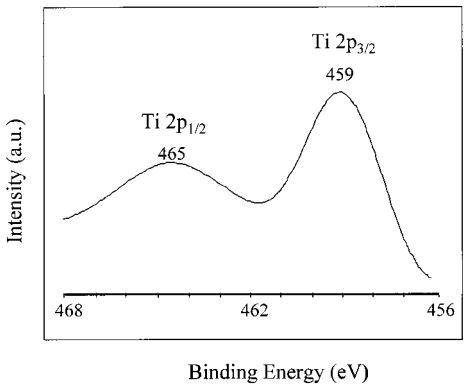

Figure 7. Ti2p X-ray photoelectron spectrum for $Eu(Ti_{0.7}Mo_{0.3})Mo_5O_{10}$.

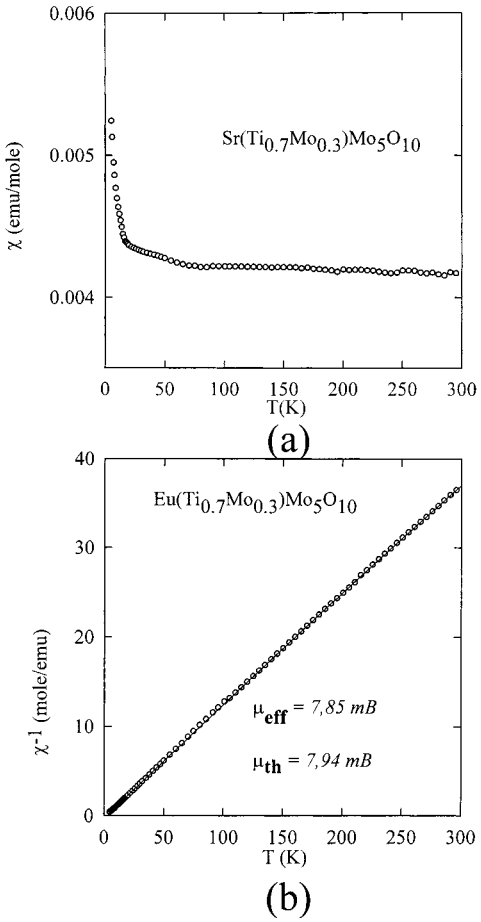

Figure 8. The temperature dependence of the molar magnetic susceptibility of $SrTi_{0.7}Mo_{0.3}Mo_5O_{10}$ and of the inverse of the molar magnetic susceptibility of $EuTi_{0.7}Mo_{0.3}Mo_5O_{10}$.

magnetic susceptibility of $EuTi_{0.7}Mo_{0.3}Mo_5O_{10}$ are shown in Figure 8. The susceptibility of the Sr compound is nearly temperature-independent in the range 100−300 K with a $\chi_{RT} = 4.3 \times 10^{-3}$ emu/mol. This behavior is consistent with the absence of localized moments on the Mo network and Ti atoms. The low-temperature upturn could be attributed to small amounts of paramagnetic impurities often present in the starting reactants. In contrast, the susceptibility data for the Eu analogue shows a strong temperature dependence (Figure 8b) according to the Curie−Weiss relation $\chi = C/(T - \theta)$ (C and θ are Curie and Weiss constants, respectively) in the entire temperature range of measurements. A least squares fitting of the observed data in the range 20−300 K resulted in $C = 7.589$ emu·K/mol and $\theta = 2.7$ K. The positive Weiss constant suggests that the exchange correlations are ferromagnetic in nature, although no magnetic ordering was evident on the Eu sublattice down to 2 K. The observed effective magnetic moment ($\mu_{eff.} = 7.85\ \mu_B$/Eu) is in good agreement with the theoretically expected value of 7.94 μ_B. This confirms that Eu is exclusively divalent (Eu^{3+} is nonmagnetic with $J = 0$) as expected from the crystallographic data and the molybdenum sublattice has no net magnetic moment.

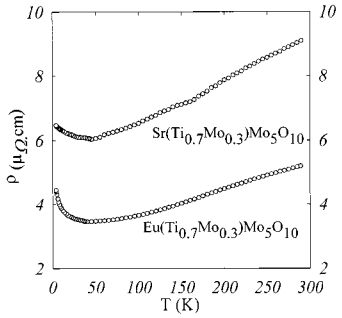

Figure 9. Temperature dependence of the electrical resistivity for the $M(Ti_{0.7}Mo_{0.3})Mo_5O_{10}$ (M = Eu, Sr) compounds.

The temperature dependencies of the electrical resistivities of the $MTi_{0.7}Mo_{0.3}Mo_5O_{10}$ (M = Sr, Eu) compounds are shown in Figure 9. Both compounds are poor metals with transitions to semiconducting states below 50 and 40 K and room temperature resistivity values of 9×10^{-3} and 5×10^{-3} Ω·cm for the Sr and Eu compounds, respectively. The poor metallic character of these compounds probably results from the positional disorder of the clusters.

In summary, we have prepared a new series of reduced molybdenum oxides $MTi_{0.7}Mo_{0.3}Mo_5O_{10}$ with M = Ca, Sr, or Eu and characterized their electrical resistivity and magnetic properties. The average structures of the Sr and Eu compounds were determined using single-crystal X-ray diffraction in space group *Pbca*. The interest in these compounds resides in the presence of bioctahedral Mo_{10} and mono- and bicapped bioctahedral Mo_{11} and Mo_{12} clusters. A metal capping mechanism was elucidated using molecular theoretical calculations. However, because of the Mo/Ti disorder it was impossible to determine whether only Mo_{10} and Mo_{12}, only Mo_{11} and Mo_{10}, or a mixture of the three species is found in these materials. No evidence was found of any superstructure or for lower symmetry. This lack of long range order makes it impossible to determine the true local structure. Consequently, additional studies by a combination of EXAFS and total neutron diffraction as used previously for Li_2MoO_3, $LiMoO_2$, and $Li_4Mo_3O_8$[25,26] would be helpful to ascertain the true local structure in these materials and determine the true nuclearity of the molybdenum clusters present in these compounds.

Acknowledgment. We thank Dr. H. Noël for the collection of the magnetic susceptibility data, Pr. W. H. McCarroll for the ICP measurements, and Dr. J.-F. Halet for his helpful comments.

Supporting Information Available: X-ray crystallographic files for $EuTi_{0.7}Mo_{0.3}Mo_5O_{10}$ and $SrTi_{0.7}Mo_{0.3}Mo_5O_{10}$, in CIF format. This material is available free of charge via the Internet at http://pubs.acs.org.

IC001209G

(25) Hibble, S. J.; Fawcett, I. D. *Inorg. Chem.* **1995**, *34*, 500.
(26) Hibble, S. J.; Fawcett, I. D.; Hannon, A. C. *Acta Crystallogr.* **1997**, *B53*, 604.